Effect of compaction and soil moisture on the effective permeability of sands for use in methane oxidation systems

van Verseveld, Charlotte J.W.; Gebert, Julia

DOI
10.1016/j.wasman.2020.03.038

Publication date
2020

Document Version
Final published version

Published in
Waste Management

Citation (APA)
van Verseveld, C. J. W., & Gebert, J. (2020). Effect of compaction and soil moisture on the effective permeability of sands for use in methane oxidation systems. *Waste Management*, *107*, 44-53. https://doi.org/10.1016/j.wasman.2020.03.038

Waste Management 107 (2020) 44–53

Contents lists available at ScienceDirect

Waste Management

journal homepage: www.elsevier.com/locate/wasman

Effect of compaction and soil moisture on the effective permeability of sands for use in methane oxidation systems

Charlotte J.W. van Verseveld, Julia Gebert *

Delft University of Technology, Department of Geoscience & Engineering, Stevinweg 1, 2628 CN Delft, the Netherlands

ARTICLE INFO

Article history:
Received 13 November 2019
Revised 16 February 2020
Accepted 28 March 2020

Keywords:
Permeability
Compaction
Soil moisture
Soil texture
Air filled porosity
Methane oxidation

ABSTRACT

Effective gas permeability is an important parameter in the design of methane oxidation systems, governing diffusive oxygen ingress and the spatial spread of landfill gas. The influences of soil texture, compaction, soil moisture and the resulting air filled porosity on the gas permeability were researched by performing pressure loss experiments on two loamy sands, currently in use as methane oxidation layer material. These experiments mimicked the influence of the intrinsic soil properties, the construction method (compaction) and the local climate (soil moisture) on the soils' permeability. In both soils, effective and specific permeability were strongly impacted by the level of soil compaction, whereas increasing moisture contents had little effect in one of the soils, only reducing effective permeability when a certain threshold was exceeded. In the other soil, structure-forming processes induced by the addition of water led to an increase in both effective and specific permeability with increasing moisture. It is concluded that the spatial spread of the landfill gas in the gas distribution layer is predominantly affected by texture and compaction of the overlying methane oxidation layer. In terms of methane oxidation system design, the choice of material and construction method have more impact on gas permeability than seasonal changes in soil moisture in moderate climates. Furthermore, air filled porosity on its own is not adequate to estimate the effective permeability of loamy sand for methane oxidation layers. Further research should address the estimation of effective gas permeability based upon soil texture, bulk density and soil moisture combined.

1. Introduction

Landfills are a major source of anthropogenic methane emissions (EPA, 2016; IPCC, 2014), resulting from the microbial degradation of waste organic matter under anaerobic conditions. One option to mitigate landfill methane emissions for which a technical treatment is no longer economically feasible is the biological oxidation in engineered methane oxidation systems. These are designed to stimulate activity of naturally occurring methanotrophic bacteria, which use methane as sole carbon and energy source (Scheutz et al., 2009). As a general principle of layout, methane oxidation systems comprise a methane oxidation layer underlain by a gas distribution layer. The main function of the methane oxidation layer is to support the methanotrophs by balancing methane and oxygen supply, providing nutrients, and maintaining an adequate water content and viable temperature regimes (Huber-Humer et al., 2008). The upper part of the methane oxidation layer also sustains vegetation, which prevents the material from being eroded, promotes soil structure formation and enables inconspicuous insertion into the landfill cover. The gas distribution layer serves to optimise the spatial homogeneity of the landfill gas fluxes entering the methane oxidation layer. Spatial homogeneity of landfill gas flow is desired to (1) prevent preferential flow paths due to which locally the landfill gas flux can become so high that these compartments are loaded beyond their oxidation capacity and that oxygen ingress is hampered, impeding methane oxidation, and (2) to tap the full spatial potential of the methane oxidation system.

According to the stoichiometry of methane oxidation, two molecules of oxygen (O_2) are needed to oxidise one molecule of methane (CH_4). The availability of oxygen is therefore of major importance for the efficiency of methane oxidation. Rannaud et al. (2009) showed with a simulation study that the oxygen penetration depth within the methane oxidation layer decreases exponentially with an increasing advection/diffusion ratio. Also, Rachor et al. (2011, 2013) and Gebert et al. (2011) found that an increased advective landfill gas bottom flux can impede the

* Corresponding author.
E-mail address: j.gebert@tudelft.nl (J. Gebert).

https://doi.org/10.1016/j.wasman.2020.03.038
0956-053X/

diffusive ingress of oxygen from the top. Additionally, the difference in effective gas permeability between the methane oxidation layer and the gas distribution layer drives the landfill gas in lateral direction (path of least resistance), creating spatial spreading of the landfill gas. Therefore, both diffusivity and effective gas permeability are important parameters in methane oxidation system design.

Diffusivity and effective gas permeability are governed by geometrical pore space characteristics such as porosity, tortuosity, connectivity and pore size distribution (Tuli et al., 2005; Poulsen et al., 2008; Gebert et al., 2011; Martínez et al., 2016) and by moisture content or air filled porosity. The pore space geometry is determined by soil texture (particle size distribution) and compaction, determining the soil's permeability (unit: m^2) which is an intrinsic property that is independent of soil moisture or the through-flowing medium. For diffusive flow, taking into account soil moisture and properties of the migrating gas leads to the property of effective gas diffusivity (unit: m^2/s), often simply termed diffusivity. With advective gas transport, the consideration of soil moisture yields the effective gas permeability (unit: m^2), if also the properties of the gas (viscosity) are considered, there is spoken of gas conductivity (unit: m/s).

The current practice of methane oxidation system design lacks adequate consideration of effective gas permeability as a design criterion to optimise spatial spread of gas flow. In this regard, two factors are of importance: (1) the influence of compaction and (2) the influence of soil moisture on effective gas permeability, reflecting the impact of construction practice (compaction) and seasonal variation in precipitation (soil moisture) on advective gas transport, respectively. Poulsen et al. (2008) researched similar relations, however, not in view of the suitability of soil material for use in methane oxidation systems. The authors observed a range where air permeability increases with increasing moisture content due to increase in the soil's level of structure. It was concluded that the common logarithm of the effective permeability appeared proportional to the common logarithm of the air filled porosity, except for intermediate values of air filled porosity, where it was inversely proportional. The more soils exhibit pronounced structure changes, the easier these regions can be observed, in general. Only two of their sample materials would be suitable for methane oxidation layers, which is a limited basis. Based upon the same data set, Poulsen and Blendstrup (2008) proposed a formula to estimate the effective air permeability from air filled porosity.

This study aimed to analyse the relationship between the effect of compaction and soil moisture on effective permeability for soils suitable for use as methane oxidation layer material under conditions of compaction and moisture typically encountered in the field situation. Secondly, the applicability of the conclusions of Poulsen et al. (2008) and Poulsen and Blendstrup (2008) for the relationship between pore space architecture and effective permeability was investigated. To this end, two soils currently in use as methane oxidation layer material in full-scale systems in the Netherlands (Geck et al., 2016; Röwer et al., 2016) and Germany (Gebert et al., 2017) were investigated using a pressure loss experiment on a soil compaction series (constant volumetric water content) and soil moisture series (constant degree of compaction). The experiment was done on such a scale that a true thickness of a methane oxidation layer was mimicked.

2. Materials and methods

2.1. Soils

The investigated sandy soils (key properties shown in Table 1) are currently used as methane oxidation layer material on two landfills. Sand 1 is used on a landfill in Hamburg (Germany), operated by Hamburg Port Authority for disposal of contaminated dredged material (Gebert et al., 2017). Sand 2 is used in an experimental methane oxidation cover on Wieringermeer landfill (The Netherlands), operated by Afvalzorg Deponie B.V. (Röwer et al., 2016; Geck et al., 2016).

2.2. Soil preparation

For each sand, nine samples were constructed, serving two experimental series: (1) Compaction series: variable compaction, constant volumetric water content, and (2) Moisture series: constant compaction, variable volumetric water content. For the compaction series, construction aimed at 75%, 80%, 85% (common point of both experiments), 90% and 95% of the Proctor density (% D_{Pr}). The volumetric water content was kept constant at the reference level corresponding to a capillary pressure of 1000 hPa at a compaction level of 85 D_{pr}, previously determined from the water retention curve of samples compacted to this level (see Section 2.8). For a compaction level <85% D_{Pr} this reference volumetric water content corresponds to a capillary pressure <1000 hPa; for a compaction level >85% D_{Pr} it corresponds to a capillary pressure >1000 hPa.

For the moisture series, the columns were constructed at different volumetric water contents corresponding to capillary pressures of 120 hPa (dryer than field capacity (60 hPa), to avoid flowing water during the experiment), 300 hPa (coarse pores drained), 1000 hPa (common point of both experiments), 3000 hPa and 15,000 hPa (permanent wilting point), while maintaining a

Table 1
Soil properties of sand 1 and 2. Su2 = slightly silty sand, St2 = slightly clayey sand (Ad-hoc AG Boden, 2005). LS = loamy sand, LFS = loamy fine sand (Benham et al., 2009). The particle diameters (d) are given in mm. The sand fractions were obtained by performing wet sieving tests according to the USDA standard (USDA MO5 2009). The proctor tests were performed according to the British Standard (BS 1377–4).

Soil property		Unit	Sand 1	Sand 2
Clay	d < 0.002 mm	[% dw]	2.6	8.8
Silt	0.002 mm < d < 0.063 mm	[% dw]	18.3	7.2
Sand	0.063 mm < d < 2.00 mm	[% dw]	79.1	82.4
Coarse	0.50 mm < d < 2.00 mm	[% dw sand]	15.9	3.4
Medium	0.25 mm < d < 0.50 mm	[% dw sand]	27.9	16.4
Fine	0.10 mm < d < 0.25 mm	[% dw sand]	45.2	75.2
Very fine	0.05 mm < d < 0.10 mm	[% dw sand]	11.0	5.0
Gravel	d > 2.00 mm	[% dw]	0	1.6
Total organic carbon (TOC)		[% dw]	1.1	1.3
$CaCO_3$		[% dw]	0	5.5
German texture class		[–]	Su2	St2
USDA texture class		[–]	LS	LFS
Proctor density D_{Pr}		[g/cm^3]	1.90	1.76
Optimum water content (w_{opt} at D_{Pr})		[% V]	10.6	13.1

constant compaction level of 85% D_{Pr}. Capillary pressure was kept constant instead of volumetric water content, because this normalises the difference in soil texture (Spokas and Bogner, 2011) and allows differentiation of the different pore size classes.

The soils were moisturised (or air-dried) to the desired water content by adding water and mixing manually, after which an incubation time of >24 h was applied, before constructing the columns.

2.3. Construction of soil in columns

The columns were constructed from PVC tubes (inner diameter = 151 mm, length = 1 m). The bottoms were sealed with a PVC cap glued around the bottom. A gas tight tube connection system was inserted at the bottom side of the column at a height of 1 cm. A 4–7 cm high gravel layer was poured into the columns to optimise the air inflow and to ensure a homogeneous spread over the base area of the column. On top, a 90 cm high soil sample was constructed in layers of 10 cm in the following order: Firstly, the mass of wet soil for 10 cm sample at intended compaction level was poured into the column. Secondly, the soil was compacted with a weight of 4.936 kg falling down multiple times (varied per sample) on a base plate with a diameter and weight of 15.1 cm and 3.359 kg, until the soil was within the 10 cm height. Thirdly, the top centimetre of the layer was scraped loose with a fork to minimise interface effects to the subsequent layer.

Dry bulk density, compaction level, volumetric water content and volumetric air content were back-calculated from wet bulk density and gravimetric water content, assuming the density of water to be 1.00 g/cm^3 and a particle specific density of 2.65 g/cm^3.

2.4. Test set-up and experimental procedures

In analogy to the falling head test known to determine the saturated hydraulic conductivity, the effective permeability was determined using a pressure loss test: air from a pressurised tank (0.514 m^3; initial pressure = 100 hPa above atmospheric pressure) was allowed to flow through the soil sample (Fig. 1), thereby equilibrating with atmospheric pressure (end pressure ~5 hPa). Tank pressure ($P_{measured}$) was measured by a calibrated pressure meter with a range of 0–100 hPa (Endress + Hauser) and recorded in high frequency (1 s). The course of its decrease over time is a function of the soil's effective permeability. All columns were tested in threefold. The set-up was checked for air-tightness and for its 'blind permeability', using a 90 cm layer of gravel. See Section 3.2 for an analysis of the reliability of the experimental procedure.

The pressure loss test is thus conducted under transient conditions. The advantage is that only one parameter (pressure) needs to be measured in contrast to a constant pressure or constant flow test where two independent devices are needed to control and/or measure pressure and gas flow rate (e.g. Groenevelt and Lemoine, 1987; McCarthy and Brown, 1992; Richard et al., 2004; Poulsen et al., 2008).

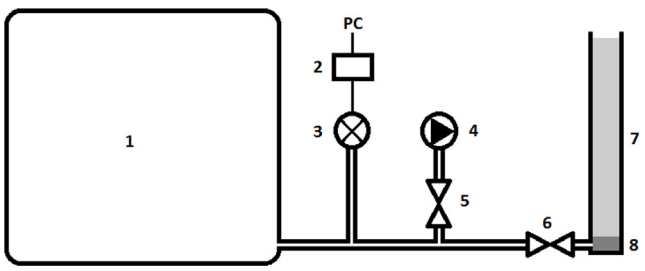

Fig. 1. Schematic representation of the test set-up: (1) tank containing (pressurised) air; (2) data logger; (3) pressure sensor; (4) compressor; (5) valve 1, open when pressurising the tank, closed during testing; (6) valve 2, closed when pressurising the tank, open during testing; (7) soil sample; (8) gravel layer.

2.5. Data evaluation and quality

The pressures and times obtained from the pressure loss test, were processed to take the tank leakage (blind test) into account. Pressure loss over time followed an exponential decay, i.e. $P = P_0\exp(-\lambda t)$. To obtain the effective permeability, an analytical formulation describing the pressure loss test was derived by equating the number of moles flowing out of the tank to the number of moles flowing into the soil column. The first can be described with the ideal gas law, assuming air at room temperature (294.15 K) and low pressure (max. 1.1 bar) behaves as an ideal gas, see the left hand side of Eq. (1). The latter can be described with Darcy's law for gas, see the right hand side of Eq. (1), since the flow is solely driven by advection as the experiment is conducted with air. Assuming that a soil can be seen as a system of tubes, the Reynolds number for this experiment is around 74 ($\ll$2000, the Reynolds number above which flow becomes transient in tubes (Bear and Cheng, 2010)) and thus Darcy's law is valid. Eq. (1) was rewritten into Eq. (2), where pressure is a function of time.

$$\frac{V}{RT}\frac{dP}{dt} = -\frac{A}{L}\frac{k_{eff}}{\mu}\frac{P}{RT}(P + P_{atm}) \tag{1}$$

$$P = \left(\frac{P_{atm}}{1 + P_{atm}/P_0 - \exp(-Ct)}\right)\exp(-Ct) \quad with\ C = P_{atm}\frac{A}{VL}\frac{k_{eff}}{\mu} \tag{2}$$

where P and P_0 = tank and starting tank pressures relative to the atmospheric pressure [P], P_{atm} = absolute atmospheric pressure [Pa], t = time relative to start of test [s], A = base area of the column [m^2], L = height of soil sample [m], V = tank volume [m^3], R = universal gas constant [J/Kmol], T = room temperature [K], μ = dynamic viscosity of air at room temperature [sPa], k_{eff} = effective permeability [m^2].

The effective permeability was obtained by fitting Eq. (2) to the processed pressures and times. Due to the influence of initial turbulent flow, data were only fitted between 80 and 5 hPa, discarding the first 20 hPa of the test. One representative value of k_{eff} was found by fitting the three experimental data sets simultaneously with DiffeRential Evolution Adaptive Metropolis (DREAM) as implemented in Matlab (The MathWorks, Inc.) by van Turnhout (2017).

By normalising the effective permeability to the fractional value of air filled porosity (ε_a [m^3/m^3]), the specific permeability (k_{spec} [m^2]) was determined (Eq. (3)) (Martínez et al., 2016):

$$k_{spec} = \frac{k_{eff}}{\varepsilon_a} \tag{3}$$

2.6. Water retention curve and pore size distribution

The water retention was determined for each of the five compaction levels of each soil using the HYPROP apparatus (METER Group, Inc.). Total porosity was determined by back-calculating the volumetric water content from the bulk density and gravimetric water content at full saturation, i.e. prior to dewatering. At the dry end, another five points were obtained using a WP4C Dewpoint PotentiaMeter (Decagon Devices). The data were hand-fitted with the Brooks and Corey (BC) model (Eqs. (4) and (5); Brooks and Corey, 1964).

$$S_{eff} = \begin{cases} (P_b/P_c)^{\lambda}, & P_c > P_b \\ 1, & P_c \leq P_b \end{cases} \quad (4)$$

$$S_{eff} = (\theta_w - \theta_{res})/(\varphi - \theta_{res}) \quad (5)$$

where S_{eff} = effective saturation [–], P_b = bubbling pressure [hPa], P_c = capillary pressure [hPa], λ = pore size distribution index [–], θ_w = volumetric water content [% V], θ_{res} = residual water content [% V], φ = total porosity [% V].

From the water retention curves, the share of different pore size classes as percentage of the total volume could be back-calculated using the formulation for the capillary pressure corresponding to the respective pore radii (Bear and Cheng, 2010):

$$P_c = 2\gamma_{wa}/R \quad (6)$$

where P_c = capillary pressure [Pa], γ_{wa} = surface tension between water and air phases [N/m], R = pore radius [m].

3. Results

3.1. Sample properties

For the compaction series (columns 1–5), dry bulk density increased upon compaction, therefore total porosity (sum of the volumetric water content and air filled porosity) decreased (Table 2). As the volumetric water content was kept constant, the change in total porosity was directly reflected by a corresponding reduction in air filled porosity. For the soil moisture series (columns 3 and 6–9), dry bulk density and thus total porosity did not change, but air filled porosity decreased with increasing volumetric water content since pore space filled with water cannot be occupied by air.

The vertical distribution of the water content was investigated by ten Bosch (2018) by means of slicing each column into discs of 10 cm thickness. Non-uniform moisture content was only observed for columns C1-8 and C1-9. Here the soil moisture in the bottom 20 cm was increased, yielding a coefficient of variation for the gravimetric water content of the entire column of 8% and 14%, respectively, while total porosity stayed constant. All other columns, including the two wettest columns of sand 2, showed good uniformity of moisture content over depth, with coefficients of variation <5%.

3.2. Evaluation of test procedure

To evaluate the magnitude of error and assess the reliability of the test procedure, three replicate soil columns were prepared for one of the samples, on each of which the permeability test was carried out three times (Fig. S1, supplementary material). The standard deviation of these tests was $1.1{\cdot}10^{-13}$ m^2 with a coefficient of variation of 2.5%, which comprises all variability in column construction and testing. The experiment is therefore highly reproducible. The effective permeability determined by each of the analytical triplicates (so for all 18 samples) differed <5% from the representative (average) k_{eff}. Conformity of analytical fits with experimental data was high at a root mean squared error of <2% of the pressure range. The effective permeability of the gravel and the test set-up were found to be $2.0{\cdot}10^{-10}$ and $1.6{\cdot}10^{-9}$ m^2, respectively, and thus did not limit the flow during the tests (see values for soils in Sections 3.3 and 3.5).

3.3. Effect of compaction on effective permeability

An increase in compaction level led to an increase in the time required for equilibrating the pressure in the tank with the atmospheric pressure (Fig. S2, supplementary material). Thus, upon increasing compaction, the soils became less permeable (values presented in Table S1, supplementary material). At comparable compaction levels, sand 1 (higher Proctor density) took more time to equilibrate pressure, indicating a lower effective permeability, than sand 2. For both sands, the effective permeability as well as the specific permeability (permeability normalised to fractional air filled porosity) showed an exponential decay with increasing bulk density (increasing compaction; Fig. 2). The decay was steeper for sand 1 than for sand 2, indicating increased susceptibility of effective permeability towards compaction. At a specific bulk density sand 1 had higher absolute values for effective permeability than sand 2.

3.4. Effect of compaction on pore size distribution

Compaction not only affects total porosity, but also induces pore size redistribution. This has an effect on both the water retention characteristics and the air filled porosity. For sand 1, compaction had the largest effect on the share of wide coarse pores (>50 μm equivalent diameter, Table 3). This fraction decreased, causing an increase in the narrow coarse pore fraction (>10–50 μ

Table 2
Physical properties for sand 1 (columns C1-x) and sand 2 (columns C2-x) for the compaction experiment (columns 1–5) and for the soil moisture experiment (columns 3 and 6–9). ρ_b = dry bulk density, *WC* = volumetric water content, *AFP* = air filled porosity.

	Column	Comp. [% D_{Pr}]	ρ_b [g/cm^3]	*WC* [% V]	*AFP* [% V]
Sand 1	C1-1	75.06	1.43	12.54	33.64
	C1-2	79.79	1.52	12.33	30.47
	C1-3	85.04	1.62	12.34	26.69
	C1-4	88.55	1.68	12.37	24.15
	C1-5	93.82	1.78	12.41	20.33
	C1-6	83.05	1.58	4.98	35.48
	C1-7	84.31	1.60	8.14	31.42
	C1-8	84.45	1.60	18.77	20.68
	C1-9	84.39	1.60	24.54	14.95
Sand 2	C2-1	74.56	1.31	20.51	29.97
	C2-2	79.52	1.40	20.12	27.07
	C2-3	84.99	1.50	20.31	23.25
	C2-4	89.53	1.58	20.68	19.86
	C2-5	95.06	1.67	19.35	17.52
	C2-6	84.96	1.50	12.46	31.12
	C2-7	85.02	1.50	16.66	26.88
	C2-8	84.99	1.50	25.55	18.00
	C2-9	84.97	1.50	30.99	12.58

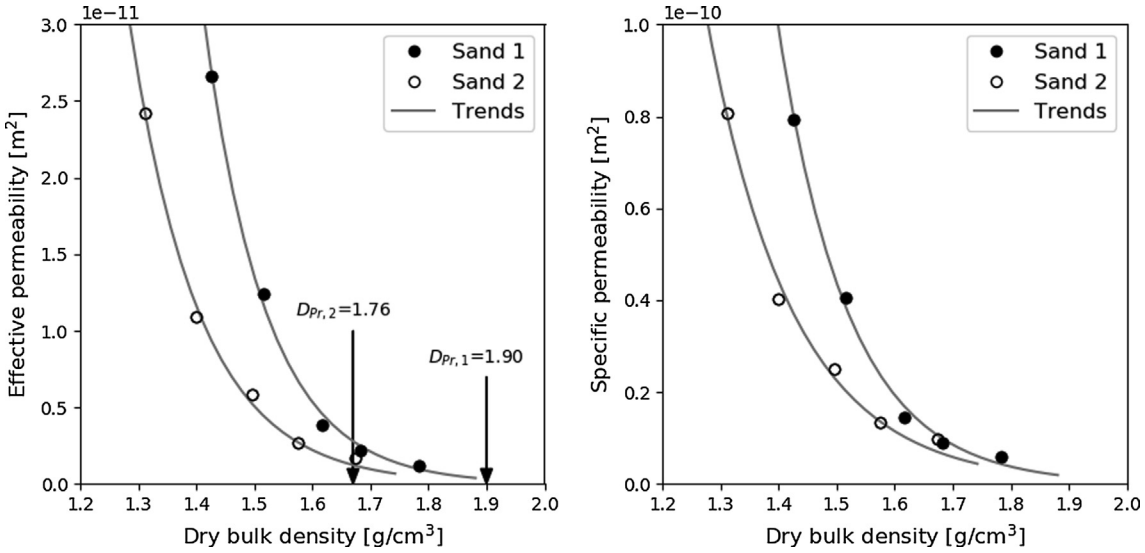

Fig. 2. Relationship between dry bulk density/compaction level and effective permeability (left) and the specific permeability (right), fitted on three analytical replicates. Arrows denote Proctor densities (D_{Pr}). No error bars presented, Coefficient of variation of experimental and analytical replicates = 2.5% of average value.

Table 3
Total porosity (φ) and pore size fractions as percentage of total volume at different compaction levels.

	Comp. [% D_{Pr}]	ρ_b [g/cm^3]	φ [% V]	*Wide coarse pore fraction* [% V]	*Narrow coarse pore fraction* [% V]	*Medium pore fraction* [% V]	*Fine pore fraction* [% V]
Size				d > 50 μm	50 > d > 10 μm	10 > d > 0.2 μm	d < 0.2 μm
Capillary pressure				Pc < 60 hPa	60 < Pc < 300 hPa	300 < Pc < 15000 hPa	Pc > 15000 hPa
Sand 1	70.38	1.34	49	31	10	4	4
	75.75	1.44	46	24	16	2	4
	79.46	1.51	43	20	16	3	4
	85.11	1.62	39	14	18	4	4
	86.92	1.65	38	11	16	7	4
Sand 2	78.81	1.39	48	35	4	0	8
	79.98	1.41	47	24	12	3	8
	83.98	1.48	44	26	10	1	8
	85.25	1.50	43	21	13	2	8
	88.42	1.56	41	10	18	5	8

m). High compaction levels also affected the narrow coarse pore fraction, resulting in a corresponding increase in the medium pore fraction (>0.2–10 μm). The fine pore fraction seemed unaffected by compaction. Sand 2 showed a similar principal response to compaction with a decrease of wide coarse pores and a corresponding increase of the narrow coarse pores. Also, some of the narrow coarse pores were compacted already at low and medium compaction levels, resulting in an increase in the medium pore fraction. Again, the fine pore fraction appeared unaffected by compaction.

In comparison, at low densities a larger wide coarse pore fraction was observed for sand 2, while at high densities sand 1 showed the larger share of wide coarse pores. Sand 2 thus showed a faster decrease of this fraction upon compaction than sand 1. However, sand 1 maintained the higher total coarse pore fraction (wide plus narrow coarse pore fraction) at all densities.

3.5. Effect of soil moisture on effective permeability

The two sands showed an opposite response of pressure loss behaviour to the level of saturation (Fig. S3, supplementary material; Fig. 3). For sand 1, an increase in volumetric water content decreased the time required for equilibrating the pressure in the tank with the atmospheric pressure. Accordingly, an increasing effective permeability was calculated upon increasing soil moisture (Table S2, supplementary material and Fig. 3, left). The specific permeability showed a similar response (Fig. 3, right). Visual inspection of the columns showed the formation of secondary macropores, likely due to the water-induced formation of soil aggregates when sand 1 was compacted at higher water contents (Fig. 4). Together, this suggests a change in pore size distribution towards larger diameter pores due to the change in water content in sand 1.

For sand 2, an increase in volumetric water content did not significantly change the time required for equilibrating the pressure in the tank with the atmospheric pressure, except for the highest water content. Accordingly, effective permeability (Table S2) showed no significant decrease upon increasing soil moisture, but dropped sharply beyond water contents of 25–30% V (Fig. 3, left). This drop corresponded to the water contents at which also the wide coarse pores began to be saturated, according to the pore size distribution inferred from the water retention curve (Table 3). Upon decreasing soil moisture, the values of the effective permeability appeared to converge to one value, which should be the value representing the intrinsic permeability valid for the respective level of compaction. Also for sand 2, an increase in specific permeability was observed with increasing soil moisture (Fig. 3, right), albeit by far not to the same extent as for sand 1. Likewise, this suggests structure-forming processes induced by water.

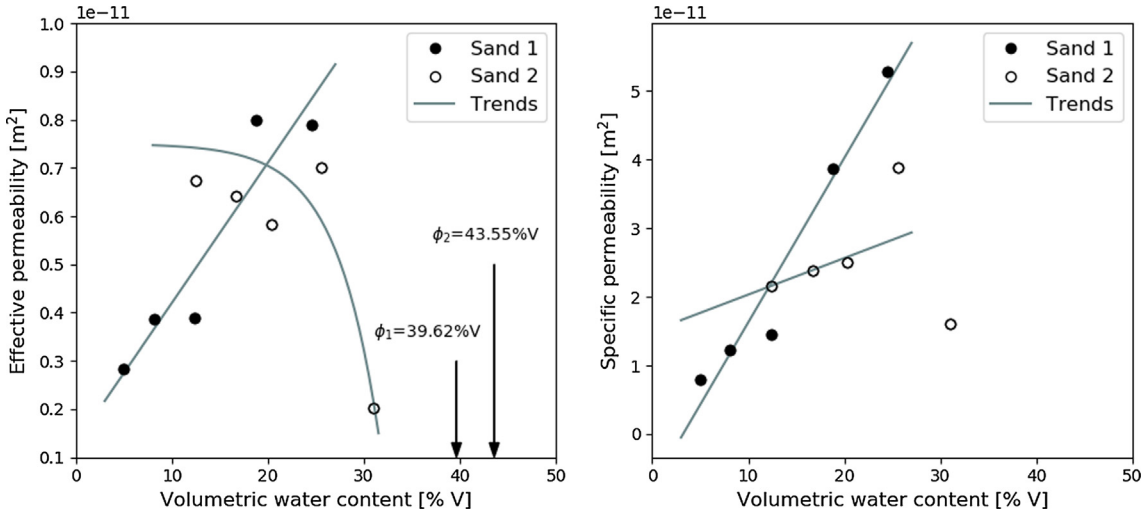

Fig. 3. Relationship between volumetric soil moisture and effective permeability (left) and specific permeability (right). Arrows denote total porosity, hence 100% saturation, for sand 1 (φ1) and sand 2 (φ2). Each point represents the average of the triple tests for a single column. No error bars presented, coefficient of variation of experimental and analytical replicates = 2.5% of average value.

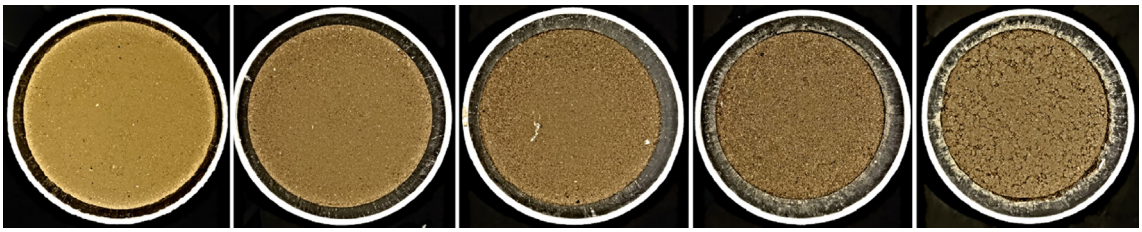

Fig. 4. Photographs of the top of the columns (Ø 151 mm) for the soil moisture experiment for sand 1. From left (dry) to right (wet): column C1-6, C1-7, C1-3, C1-8, C1-9.

3.6. Effect of air filled porosity on the effective permeability

In the soil compaction experiment, effective permeability increased exponentially with decreasing compaction level for both soils (Fig. 5). This trend was also seen for the specific permeability, demonstrating a higher advective gas transport efficiency with increasing air filled porosity. In the soil moisture experiment, on the other hand, effective permeability and specific permeability for sand 2 converged to one value, i.e. were largely independent of the extent of air filled porosity once moisture was decreased below a threshold. For sand 1, the soil moisture experiment showed an opposite trend, where both the effective and the specific permeability increased with decreasing air filled porosity (increasing moisture), concomitant with the structure forming processes observed for this soil (Fig. 4).

Overall, effective permeability reacted more strongly to changes in compaction than to changes in moisture. In brief, the effective permeability of the same soil varied for a given value of air filled porosity, depending on whether porosity was impacted by compaction level or soil moisture. When comparing the two soils, it was seen that at similar air filled porosity sand 2 had a higher effective permeability than sand 1.

4. Discussion

4.1. Effect of soil compaction on permeability

The two investigated soils showed a similar level of effective permeability as well as a similar response to compaction. The general similarity can be explained by the similarities in particle size distribution, as both sands have comparable shares of the sand fraction (Table 1). Their values found for the effective permeability are well within ranges found in literature for loamy sands: 10^{-8}–10^{-14} m^2 (Warrick, 2002; Lu and Likos, 2004). They are also in the same order as the values previously found for sand 2 by Geck (2017) and for the sands tested in a similar experiment by Poulsen et al. (2008).

Advective air transport in unsaturated soils is most effectively facilitated through the network of large diameter (coarse) pores (see law of Hagen-Poiseuille), which are particularly sensitive to compaction (see Table 3; also Gebert et al., 2011; Gebhardt et al., 2009). Therefore, gas effective permeability strongly depends on matrix pore geometry, thus on compaction, and on soil structure forming processes, inducing secondary macropores (Moldrup et al., 2001).

Effective permeability decreased exponentially with increasing bulk density, thus with increasing level of compaction. The exponential decay, also found by Gebert et al. (2009) and (Geck, 2017), implies that initial compaction has a large influence on the effective permeability, while upon further compaction this influence reduces. This can be explained by the pore size redistribution. In both sands, mainly the share of wide coarse pores was decreased upon compaction, where the share of narrow coarse pores was increased (Table 3). In total, the coarse pores (>10 μm) were decreased. The medium pore fraction showed a small increase, while the fine pore fraction remained unaffected by the compaction. This is in accordance with Moldrup et al. (2001), Richard et al. (2001), Gebhardt et al. (2009), Wickramarachchi et al. (2011) and Gebert et al. (2011). Overall this means that initial compaction particularly affects the coarse pores and therefore the effective permeability decreases fast. Upon further compaction, the

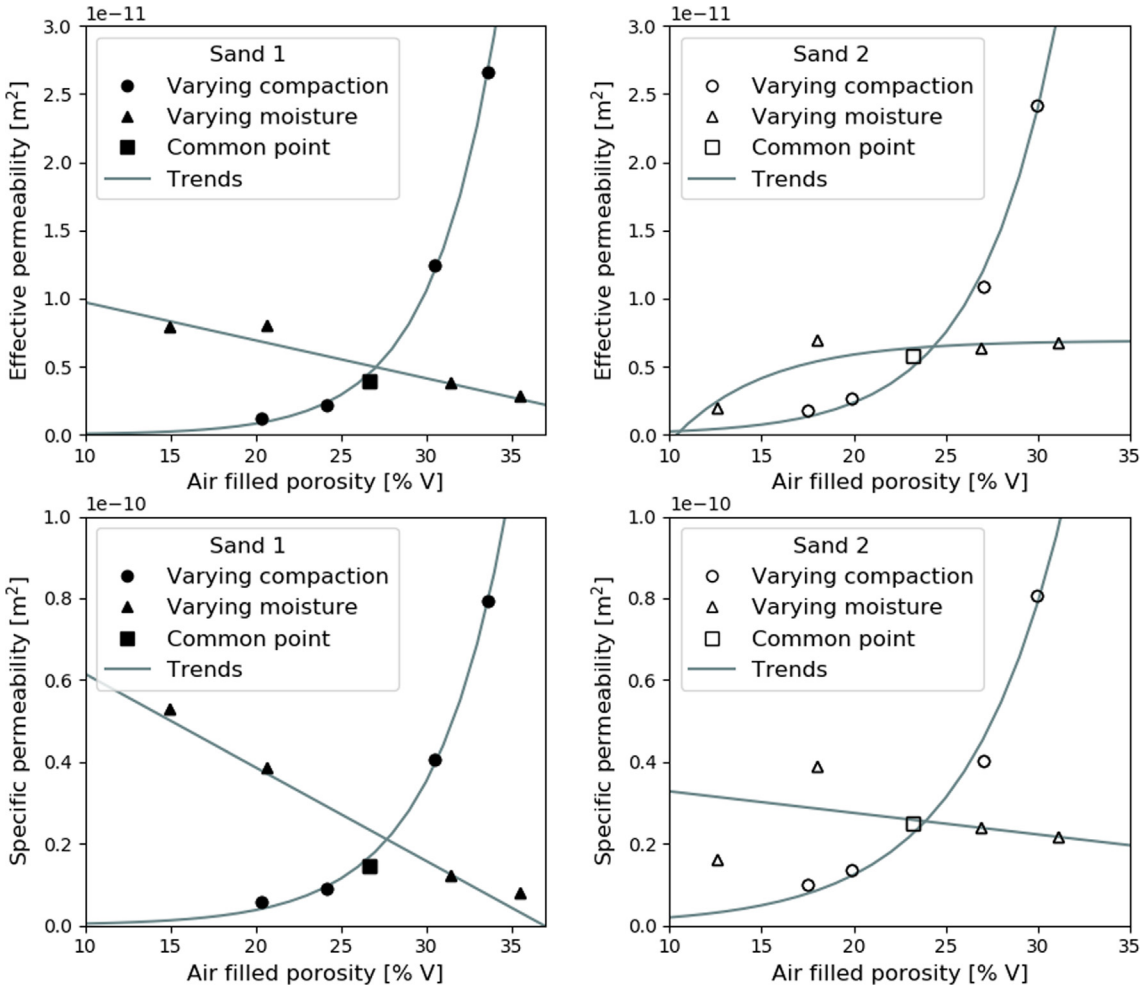

Fig. 5. Relationship between effective and specific permeability and air filled porosity for sand 1 (left) and sand 2 (right) for varying compaction level and soil moisture. Each point represents the average of the triple tests for a single column. No error bars presented, coefficient of variation of experimental and analytical replicates = 2.5% of average value.

share of compactible coarse pores decreases and thus the decrease in the effective permeability slows down, possibly adding to the observed exponential decay.

Sand 2 had the higher share of wide coarse pores below a bulk density of 1.5 g/cm^3 (Table 3), which would indicate that below this bulk density sand 2 should have the higher effective permeability. Instead the data showed that at all bulk densities sand 1 had the higher effective permeability. Sand 1 had at all bulk densities the highest total coarse pore fraction, and at the same time part of the narrow coarse pores of sand 2 were filled with water. This shows that in addition to what Gebert et al. (2011) stated, also the narrow coarse pores have a dominant effect on the effective permeability of a soil, provided that they are drained.

With respect to soil texture, it is seen that sand 1 had slightly more fines and a better graded sand fraction than sand 2 (Table 1). Both aspects promote compactibility, which is also confirmed by the higher Proctor density found for sand 1. Therefore, the effective permeability of sand 1 was expected to be influenced more by compaction than that of sand 2, which indeed was the case (Fig. 2). Deepagoda et al. (2010) found that at a given matric potential, dense soils are less permeable than less dense soils, due to the reduced air filled porosity as a result of the increased water retention, which corresponds with the results in this paper. This demonstrates the bilateral impact of compaction: Firstly, upon compaction, the volumetric share of solids is increased, leading to decreased air filled porosity. Secondly, compaction redistributes the pore sizes at the cost of the coarse pores, which enhances water retention, leading to a higher soil moisture content at a certain matric potential.

4.2. Effect of soil moisture on permeability

Following the law of capillarity (Young-Laplace), increasing soil moisture will fill fine pores first while the remaining air filled pore system consists of the coarser pores. The connectivity of the pore system is impeded when the soil moisture increases beyond a certain threshold. This critical soil moisture corresponds to the air content at the threshold of occlusion to gas migration (θ_{occ}), as proposed by Ahoughalandari and Cabral (2017). The effect was indeed seen for soil 2 where increasing soil moisture led to only a slight decrease in effective permeability, and to a slight increase in specific permeability, followed by a sudden drop. The slight decrease is attributed to the finer pores contributing least to gas transport being filled first due to larger capillary suction, while the coarse ones contributing most to gas transport are saturated last. With decreasing soil moisture, effective permeability appeared to converge to one value, which should be the intrinsic permeability for the specific compaction level. The concurrent increase in specific permeability with increasing moisture content, albeit small in effect, indicates that with increasing soil moisture the efficiency

of gas transport increased. This suggests structure-forming processes as a result of increasing soil moisture, inducing macroporosity. Larger diameter pores allow for more effective advective gas transport as advective gas transport is proportional to the 4th power of the pore radius (law of Hagen-Poiseuille). The drop in effective permeability only took place beyond a certain threshold value for the soil moisture. Beyond this point, water menisci forming in pore throats impede the connectivity of the most effective air filled pore space, the large diameter pores, thus decreasing the effective permeability. For sand 2, this point was reached before the sand was fully saturated. The threshold soil moisture was between 26 and 31% V, which at the given bulk density equalled a gravimetric water content of 17–21% dw. For permeability, the only values reported for this threshold are 85% saturation for a clay (Jucá and Maciel, 2006) and around saturation for several sandy or silty loams (Tuli et al., 2005). For the experiments reported here, the drop took place already around 65% saturation. The soils used in the referenced works are much more finely textured and hence have a higher field capacity in relation to air capacity than the soils investigated in this study. It is therefore plausible that the threshold levels were higher. Rachor et al. (2013) found this threshold to occur around field capacity in a field experiment. Beyond saturation around field capacity, i.e. upon saturation of wide coarse pores, gas emissions from a landfill surface sharply dropped. The field capacities of sand 2 was 32% V, the threshold hence occurring slightly below its field capacity.

In contrast, increasing soil moisture in soil 1 led to an increase in effective permeability, rather than to a decrease. Also, a far greater increase in specific permeability was observed. This effect was reported previously (Poulsen et al., 2008; Richard et al., 2004) and was attributed to the water-facilitated aggregation of fines into fewer larger particles, resulting in increased inter-aggregate pore sizes. The larger share of coarse pores increased the effective permeability. In this study, visual inspection indeed revealed aggregates and hence larger pores to form for the columns containing sand 1 adjusted to elevated moisture content before compaction (Fig. 4). Therefore, the trend of increasing effective permeability with increasing water content seen for sand 1 (and to a lesser extent also for sand 2) is assumed to be due to the water-enhanced aggregation of fines. Complimentary, the non-uniform water distribution of the two wettest columns of sand 1 was expected to form a barrier, leading to lower permeability. The fact that they actually showed a higher permeability, strengthens the hypothesis of the water-induced aggregation. The reason for this behaviour possibly lies within the mineralogy of the fine fraction of this sand and should be further investigated. For sand 1, the threshold beyond which soil moisture curbs advective gas transport, as seen for sand 2, was not reached in this experiment.

The trends found in this study fit well with those found by Poulsen et al. (2008) for their two investigated natural sands. Three observations can be made: Firstly, the range of investigated air filled porosity falls within the boundary ranges of the Hjorring fine sand (Fig. S4, supplementary material); secondly, the compaction series fits the log-linear trends also found by Poulsen et al. (2008) for the relationship between air filled porosity and effective permeability (Fig. 5); thirdly, both the decreasing and increasing trend of the effective permeability with increasing moisture is also seen for the natural sands investigated by Poulsen et al. (2008). The data were also fitted using the predictive model proposed by Poulsen and Blendstrup (2008). This did not yield too accurate prediction of the effective gas permeability (errors up to a factor of 10 and the trend was not always correct) and accuracy of the fit was highly influenced by the concrete data points used to perform the fit. Furthermore, the fitting requires upfront knowledge if the trend of the change is proportional or inversely proportional (due to structure formation) with increasing water content. As the effect of moisture on soil structure formation cannot be easily inferred upfront, it is recommended to perform more elaborate research on the estimation of the effective gas permeability for the relatively small range of sands suitable for methane oxidation systems.

4.3. Comparison of effects of compaction and moisture and of individual soils

The results from the compaction series and the moisture series show that at one single value for air filled porosity the effective permeability of a sand can vary due to the combined effects of compaction and soil moisture. This is attributed to the difference in connectivity, tortuosity and pore size distribution at similar air filled porosity. Moldrup et al. (2001) concluded that for the gaseous phase transport tortuosity is mainly related to the connectivity of the air filled pores. So, the different values for effective permeability at a single air filled porosity are attributed to the difference in connectivity and pore size distribution. From Fig. 5 in combination with Table 3 it can be seen that at for instance 20% V air filled porosity the soil was at a denser and dryer state for the compaction experiment, i.e. more smaller pores, which were quite well connected, but did not contribute too much to advection. For the soil moisture experiment the soil was at a looser and wetter state, i.e. more larger pores, where the smaller pores were filled with water and the larger pores were still quite well connected. The result was that the soil moisture series yielded a higher effective permeability at this end of the graph than the compaction series. At higher bulk densities the air filled porosity became so low, that there were no coarse pores anymore, thus impeding advection, or the soil became too wet, impeding connectivity of the air filled pore system. On the other end of the graph, for instance at 30% V air filled porosity, the soil was in a looser but wetter state for the compaction experiment, where the soil of soil moisture series was in a denser but dryer state. The soil of the compaction series now had a greater share of well-connected coarse pores. The soil of the soil moisture series has less coarse pores, but a larger part of the medium pores were air filled as well. However, the medium pores do not contribute that much to advection, thus the compaction line has a higher effective permeability. These effects are seen irrespectively of the trend of the moisture experiment.

Moldrup et al. (2000) emphasised the importance of taking into account the effects of changing pore shape and configuration in a wet soil compared to a dry soil. Comparing the two sands of this study shows that sand 2 had the higher effective permeability at similar air filled porosity for the compaction experiment. At the same air filled porosity, sand 1 was denser and dryer, while sand 2 was looser and wetter, which caused sand 2 to have more well-connected coarse pores, while sand 1 had more medium pores which did not contribute as much to advection. A similar difference in effective gas permeability for two different kinds of gravel at the same air filled porosity was found by Wickramarachchi et al. (2011).

The discussed findings indicate that at any given air filled porosity both the effective and the specific permeability can vary for different soils. Moreover, they can also vary for the same soil, depending on the combination of compaction and moisture content leading to the respective level of air filled porosity. In these experiments, for a single soil the effective permeability varied with a factor of up to 27, which on a scale of the range of possible permeability values for different soil textures and bulk densities is not much, but could have an serious impact on the spatial spread of gas and hence on the performance of the methane oxidation system. This means that air filled porosity on its own may not be an adequate proxy of effective permeability in light of methane oxidation system design.

Lastly, the data of the two experiments showed that for these loamy sands, compaction has a larger influence on the effective

permeability than soil moisture, within the boundaries tested in the experiments. Especially in more coarsely textured soils, such as the investigated sands, soil moisture may become significant for effective permeability only at high levels of saturation. Permeability of more finely textured materials, i.e. silt- or clay dominated soils, will be more sensitive to soil moisture as the share of larger diameter pores is much lower already at comparable bulk densities. This means that soil texture, determining compactibility and corresponding pore architecture, and actual compaction of the methane oxidation layer will significantly affect the spatial spread of landfill gas in the gas distribution layer. From the perspective of optimal gas distribution a high difference in permeability between the methane oxidation and the gas distribution layer, i.e. a higher compaction of the methane oxidation layer, is preferred. This, however, conflicts with the demands on diffusive oxygen ingress, governed by the soil's diffusivity, which is negatively affected by compaction (Rachor et al., 2011). The art of good methane oxidation system design hence lies within finding the optimal balance between spatial landfill gas distribution and oxygen ingress to obtain maximum oxidation capacity.

It must be kept in mind that soil texture and the temporary soil moisture during construction have an influence on the ease of compaction (Sanchez-Giron et al., 1998) and should thus be taken into account when determining the construction method.

5. Conclusions

The effective gas permeability of the gas distribution and methane oxidation layers is a key parameter in methane oxidation system design, because it impacts the spatial distribution of the landfill gas load within the gas distribution layer and hence determines the load per unit area. The influence of soil texture, compaction, soil moisture, and the corresponding levels of air filled porosity on the effective and specific gas permeability were researched using pressure loss experiments on two types of sand that are currently in use in full scale methane oxidation systems. An analytical formulation was derived to fit the experimental data, based upon Darcy's law and the ideal gas law. The results revealed distinct trends.

At similar air filled porosity, effective and specific gas permeability can vary for the same soil depending on the compaction level and water content and their influence on the connectivity and tortuosity of the air filled pore system. Also, they can vary between soils depending on the soil texture. Air filled porosity on its own is thus not a suitable indicator for deriving effective gas permeability in light of methane oxidation system design. The predictive model proposed by Poulsen et al. (2008) was not sufficient to accurately predict effective permeability in the small range of sands suitable for methane oxidation systems (in relation to the large range of possible sol particle size distributions). Further research should be conducted to establish a relationship to derive values for the effective gas permeability from soil texture, bulk density and water content combined for these types of sands. Compaction mainly affected effective permeability through the reduction of the share of the wider diameter pores, most responsible for the efficiency of advective gas transport. This was suggested by the decrease in the share of coarse pores inferred from the water retention curves for the different compaction levels and further evidenced by the exponential decrease in specific permeability. The latter indicates a strong reduction in the efficiency of the gas transporting pore system after compaction.

Varying the soil moisture led to variable responses of the two sands with respect to the effective and specific permeability. Both an increase as a decrease in effective and specific permeability with increasing soil moisture and with the resulting decreasing air filled porosity were observed. Water-induced aggregation, even in sand-dominated soils, is suspected to cause inter-aggregate macropores which enhance advective transport processes. This is suspected to be the cause of the observed increase of specific permeability with increasing moisture content, which could be seen in both soils. The mineralogy of the clay fraction, even in soils with low clay contents such as the researched ones, is assumed to be relevant for these structuring processes. It is therefore suggested to include analysis of aggregate formation in future research of other materials which are candidates for methane oxidation systems. Soil moisture exceeding the threshold value beyond which throats of the wider diameter pores (most effective for advective gas transport) are blocked, is most relevant for the reduction in effective permeability, as seen for soil 2. For soil 1, this threshold was not reached by the investigated moisture range.

Overall, the effective gas permeabilities were in the same range as found by other authors and the general effect of compaction and moisture on air filled porosity and effective permeability follow the trends from Poulsen et al. (2008) for two investigated natural sands.

Irrespective of the effects of soil moisture on structure formation, seen in both soils, it is concluded that for the investigated loamy sands and within the boundaries of compaction and moisture levels tested, compaction through its effect on pore size redistribution (reduction of wider diameter pores) has a much larger influence on the effective permeability than soil moisture. Furthermore, soil texture influences the sensitivity of the gas permeability to varying compaction and water content. Therefore it can be concluded that soil texture and compaction predominantly influence the effective gas permeability and will thus affect the spatial spread of the landfill gas in the gas distribution layer.

In terms of methane oxidation system design, the influences of choice of material and construction method (type of vehicle, surface load) will have a more pronounced influence on the effective gas permeability and thus on the spatial spread of landfill gas in the gas distribution layer, than seasonal changes in saturation levels in moderate climates.

Declaration of Competing Interest

The authors declare that they have no known competing financial interests or personal relationships that could have appeared to influence the work reported in this paper.

Acknowledgements

The authors would like to thank Hamburg Port Authority and Afvalzorg Deponie B.V. for their support with soil sampling, soil transport and the fruitful discussions.

Funding sources

This research did not receive any specific grant from funding agencies in the public, commercial, or not-for-profit sectors.

Appendix A. Supplementary data

Supplementary data to this article can be found online at https://doi.org/10.1016/j.wasman.2020.03.038.

References

Ad-hoc AG Boden, 2005. Bodenkundliche Kartieranleitung. 5. Auflage. Bundesanstalt für Geowissenschaften und Rohstoffe und Geologische Landesämter der Bundesrepublik Deutschland, Schweitzerbartsche Verlagsbuchhandlung, Stuttgart.

Ahoughalandari, B., Cabral, A., 2017. Influence of capillary barrier effect on biogas distribution at the base of passive methane oxidation biosystems: Parametric study. Waste Manage. 62, 162–187.
Bear, J., Cheng, A.H.D., 2010. Modeling Groundwater Flow and Contaminant Transport, Vol. 23. Springer Science & Business Media.
Benham, E., Ahrens, R., Nettleton, W., 2009. Attachment to MO5 Soil Technical Note-16. National Soil Survey Center, USDA-NRCS, Lincoln, Nebraska.
Brooks, R., Corey, T., 1964. Hydraulic properties of porous media. Hydrology Papers, Colorado State Univ. 24, 37.
Deepagoda, T.K.K., Moldrup, P., Schjønning, P., Jonge, L.W.D., Kawamoto, K., Komatsu, T., 2010. Density-corrected models for gas diffusivity and air permeability in unsaturated soil. Vadose Zone J. 10 (1), 226–238.
EPA, 2016. Inventory of U.S. Greenhouse Gas Emissions and Sinks. Technical report, United States Environmental Protection Agency.
Gebert, J., Groengroeft, A., Pfeiffer, E.M., 2011. Relevance of soil physical properties for the microbial oxidation of methane in landfill covers. Soil Biol. Biochem. 43 (9), 1759–1767.
Gebert, J., Kleinschmidt, V., Gröngröft, A., 2009. Gas Permeability Tests – Development of Procedures and Analysis of 9 Materials. University of Hamburg.
Gebert, J., Harms, C., Steinert, B., 2017. Full-scale implementation of methane oxidation windows on a mono-landfill: technical design and monitoring concept. 15. International Waste Management and Landfill Symposium (Sardinia 2015). CISA Publisher.
Gebhardt, S., Fleige, H., Horn, R., 2009. Effect of compaction on pore functions of soils in a Saalean moraine landscape in North Germany. J. Plant Nutr. Soil Sci. 172 (5), 688–695.
Geck, C., 2017. Temporal and Spatial Variability of Soil Gas Transport Parameters, Soil Gas Composition and Gas Fluxes in Methane Oxidation Systems. University of Hamburg.
Geck, C., Scharff, H., Pfeiffer, E.M., Gebert, J., 2016. Validation of a simple model to predict the performance of methane oxidation systems, using field data from a large scale biocover test field. Waste Manage. 56, 280–289.
Groenevelt, P., Lemoine, G.G., 1987. On the measurement of air permeability. Netherlands J. Agric. Sci. 35 (3), 385–394.
Huber-Humer, M., Gebert, J., Hilger, H.A., 2008. Biotic systems to mitigate landfill methane emissions. Waste Manage. Res. 26 (1), 33–46.
IPCC, 2014. Fifth Assessment Report. Technical report, International Panel on Climate Change.
Jucá, J.F.T., Maciel, F.J., 2006. Gas permeability of a compacted soil used in a landfill cover layer. In: Unsaturated Soils 2006, pp. 1535–1546.
Lu, N., Likos, W.J., 2004. Unsaturated Soil Mechanics. Wiley.
Martínez, I., Chervet, A., Weisskopf, P., Sturny, W.G., Rek, J., Keller, T., 2016. Two decades of no-till in the Oberacker long-term field experiment: Part II. Soil porosity and gas transport parameters. Soil Tillage Res. 163, 130–140.
McCarthy, K.P., Brown, K.W., 1992. Soil gas permeability as influenced by soil gas-filled porosity. Soil Sci. Soc. Am. J. 56 (4), 997–1003.
Moldrup, P., Olesen, T., Gamst, J., Schjønning, P., Yamaguchi, T., Rolston, D.E., 2000. Predicting the gas diffusion coefficient in repacked soil water-induced linear reduction model. Soil Sci. Soc. Am. J. 64 (5), 1588–1594.
Moldrup, P., Olesen, T., Komatsu, T., Schjønning, P., Rolston, D.E., 2001. Tortuosity, diffusivity, and permeability in the soil liquid and gaseous phases. Soil Sci. Soc. Am. J. 65 (3), 613–623.
Poulsen, T.G., Blendstrup, H., 2008. Predicting air permeability in porous media with variable structure, bulk density, and water content. Vadose Zone J. 7 (4), 1269–1275.
Poulsen, T.G., Blendstrup, H., Schjønning, P., 2008. Air permeability in repacked porous media with variable structure-forming potential. Vadose Zone J. 7 (4), 1139–1143.
Rachor, I., Gebert, J., Gröngröft, A., Pfeiffer, E.M., 2011. Assessment of the methane oxidation capacity of compacted soils intended for use as landfill cover materials. Waste Manage. 31 (5), 833–842.
Rachor, I.M., Gebert, J., Gröngröft, A., Pfeiffer, E.M., 2013. Variability of methane emissions from an old landfill over different time-scales. Eur. J. Soil Sci. 64 (1), 16–26.
Rannaud, D., Cabral, A., Allaire, S.E., 2009. Modeling methane migration and oxidation in landfill cover materials with TOUGH2-LGM. Water Air Soil Pollut. 198 (1–4), 253.
Richard, G., Cousin, I., Sillon, J.F., Bruand, A., Guérif, J., 2001. Effect of compaction on the porosity of a silty soil: influence on unsaturated hydraulic properties. Eur. J. Soil Sci. 52 (1), 49–58.
Richard, T.L., Veeken, A.H., de Wilde, V., Hamelers, H.V.M., 2004. Air-filled porosity and permeability relationships during solid-state fermentation. Biotechnol. Prog. 20 (5), 1372–1381.
Röwer, I.U., Scharff, H., Pfeiffer, E.M., Gebert, J., 2016. Optimized landfill biocover for CH_4 oxidation I: experimental design and oxidation performance. Curr. Environ. Eng. 3 (2), 80–93.
Sanchez-Giron, V., Andreu, E., Hernanz, J.L., 1998. Response of five types of soil to simulated compaction in the form of confined uniaxial compression tests. Soil Tillage Res. 48 (1–2), 37–50.
Scheutz, C., Kjeldsen, P., Bogner, J.E., De Visscher, A., Gebert, J., Hilger, H.A., Huber-Humer, M., Spokas, K., 2009. Microbial methane oxidation processes and technologies for mitigation of landfill gas emissions. Waste Manage. Res. 27 (5), 409–455.
Spokas, K.A., Bogner, J.E., 2011. Limits and dynamics of methane oxidation in landfill cover soils. Waste Manage. 31 (5), 823–832.
Ten Bosch, S., 2018. Spatial variability of physical soil properties in constructed columns BSc thesis. Delft University of Technology.
Tuli, A., Hopmans, J.W., Rolston, D.E., Moldrup, P., 2005. Comparison of air and water permeability between disturbed and undisturbed soils. Soil Sci. Soc. Am. J. 69 (5), 1361–1371.
Van Turnhout, A., 2017. Characterizing Dominant Processes in Landfills to Quantify the Emission Potential. Delft University of Technology.
Warrick, A., 2002. Soil Physics Companion. CRC Press, Taylor & Francis Group.
Wickramarachchi, P., Kawamoto, K., Hamamoto, S., Nagamori, M., Moldrup, P., Komatsu, T., 2011. Effects of dry bulk density and particle size fraction on gas transport parameters in variably saturated landfill cover soil. Waste Manage. 31 (12), 2464–2472.